Dispatchability of Solar Photovoltaics from Thermochemical Energy Storage

R. Fernández [a], C. Ortiz [b,*], R. Chacartegui [a], J.M. Valverde [b], J.A. Becerra [a]

[a] Escuela Técnica Superior de Ingeniería, Universidad de Sevilla, Camino de los descubrimientos s/n, 41092 Sevilla, España
[b] Facultad de Física, Universidad de Sevilla, Avenida Reina Mercedes s/n, 41012 Sevilla, España,
[*] Corresponding author (C. Ortiz): cortiz7@us.es; t:(+34) 655783930

Abstract

Solar photovoltaic plants are today a competitive alternative to power plants based on fossil fuels. Cost reduction in photovoltaics modules, scalability and ease of installation of these plants are enabling a rapid worldwide expansion of the technology. Nevertheless, the dispatchability still remains as the major challenge to overcome due the intrinsic variability of solar energy. Most of the current solar photovoltaic facilities at large scale lack energy storage while those with storage systems rely on expensive batteries. Batteries are based on elements such as nickel, lithium or cadmium whose scarcity hinder the sustainability of batteries for storing energy in the large scale. This manuscript presents a novel concept to integrate thermochemical energy storage in photovoltaic plants. Furthermore, the concept is also directly adaptable to wind power plants to store surplus energy. The paper analyses the suitability of the Calcium-Looping process as thermochemical energy storage system in solar photovoltaics plants. The system works as follows: a part of power produced in the solar plant provides electricity to the grid while the rest is used to supply the heat for calcination of calcium carbonate. After calcination, the products of the reaction – calcium oxide and carbon dioxide- are stored separately. When power production is required, the stored products are brought together in a carbonation reactor wherein the exothermic reaction releases energy for power production. The overall system is simulated to estimate the process behaviour and results show that storage efficiencies of ~40% can be achieved. Moreover, an economic analysis is developed to compare the proposed system with batteries. Limestone is abundant, cheap and non-toxic, which are essential requirements for a massive storage of energy. Due to the low price of natural calcium oxide precursors, such as limestone, and the expected longer lifetime of equipment than batteries, the Calcium-Looping process can be considered as a potential alternative for improving dispatchability in solar photovoltaic plants.

Keywords

Renewable energy, Solar Photovoltaics (PV), Thermochemical Energy Storage (TCES), Calcium looping (CaL), Dispatchability

1. Introduction

Solar photovoltaics (PV) plants are one of the most promising markets in the field of renewable energy [1], with a PV market growth year-on-year of 29% in 2017 [2]. The size of PV Plants varies depending on the application [3]: from Pico PV systems of few watts used for off-grid basic electrification, to Grid Connected Centralized systems in the range of MWs [4]. The scalability (from kW to MW), ease of installation and cost reduction are enabling a fast growing of the PV installed power all around the world, representing the third worldwide

largest renewable source after hydro and wind [5]. Technical improvements and economy of scale have resulted in a significant cost reduction of solar photovoltaic (PV) modules, and an intense global growth of PV industry [6]. Nevertheless, dispatchability still remains as a major challenge to be solved due to intrinsic variability of solar energy. The intermittent nature of PV can also cause oscillations in the power system's voltage and frequency, which create new challenges for the integration of PV in the electric power system [7]. Integrating grid connected PV plants to energy storage systems is a possible solution to solve this problem [8], making it possible to combine production and demand to optimize the operation of plants.

Batteries -Electrochemical Energy Storage Systems (ECES)- have been postulated as the best positioned systems for solving dispatchability in PV plants. There are several battery types available for the power sector. Sodium sulphur is the predominant technology although in the last years the market is shifting to lithium-ion batteries since they provide higher energy and power density, longer durability and lower cost. Other possibilities are advanced lead-acid, redox flow or Nickel Cadmium [9]. Rydh et al. [10] reported the energy efficiency of different large scale energy storage technologies based on batteries that are currently gaining attention ranging between 85-95% for Li-ion batteries to 60-65% for Polysulfide-Bromine (PSB) technology (a redox flow battery) [9]. A comprehensive review on batteries for energy storage can be found in [11]. Despite the huge expansion of batteries in the market [1], the commercial expansion of batteries still faces great challenges for large scale energy storage. Batteries are based on materials such as Lithium, Nickel or Cobalt, whose scarcity and environmental impact compromise the technical and economic viability of this technology for a massive energy storage around the world. Moreover, the cost of batteries (around 300-550$/kWh) is a major drawback [9] being one order of magnitude higher than thermal storage systems. Recently Tesla has built a Li-ion battery (100MW/129MWh) to demonstrate large scale penetration of RES in Australia [12]. By 2030 the expected PV installed capacity will be nine times higher than in 2013 [9]. In this line, Geth el al. [13] highlight the necessity of large scale storage systems for integrating non-dispatchable renewable energy and exclude battery storage as a realistic candidate to provide bulk energy storage capabilities. In addition to resource scarcity and cost, another major challenge of batteries is to prolong the lifetime of the system. Because of the variability of solar input, batteries are subjected to continuous charge and discharge cycles, which increases their complexity and cost for large scale facilities [9]. Due to these serious drawbacks most of the PV facilities do not include energy storage systems. Batteries worldwide installed storage capacity is less than 0.5% of the total storage capacity for electrical energy

The most extended system at commercial scale for large scale energy storage is pumped hydro, which accounts for 99% of the total installed energy stored [14]. Pumped hydro is certainly a cheap and feasible solution for the massive storage of energy [15]. However, the application of this technology is constrained to locations with high altitude gradients. A notably a smaller number of facilities use Compressed Air Energy Storage (CAES) systems with a worldwide installed storage capacity for electrical energy around 0.35%. CAES is also a commercial alternative with demonstration plants operating for years [14]. There are other solutions for large scale electrical energy storage not yet fully developed at the commercial scale which are based on diverse methods such as the flywheel technology [16], superconducting magnetic energy storage [17] or supercapacitors energy storage [18].

Remarkably, the challenge of a massive deployment of energy storage systems at large scale will require the use of abundant, cheap and non-toxic materials. In this line, this manuscript

presents a novel concept to integrate Thermochemical Energy Storage (TCES) systems in PV plants, as a sustainable and large-scale storage system. A large number of TCES systems have been proposed in the last years [19], most of them to be applicable in CSP plants [20]. However, few works report the use of electrical energy to carry out the endothermic reaction in order to improve dispatchability in PV plants. Li and Hao [21] proposed a methanol-based TCES system to be integrated in PV plants. This system is based on the use of waste-heat from the PV cell to carry out the endothermic methanol decomposition. Solar-to-electric efficiencies of 41% [22] and 43% [21] were reported in different works.

Among the TCES systems, the Calcium-Looping (CaL) process, based on the multicyclic calcination/carbonation of calcium carbonate ($CaCO_3$) has been selected in this work. The CaL process has been recently analysed to enhance dispatchability in Concentrating Solar Power (CSP) plants [23]. Main advantages of the CaL process for TCES are: i) the high energy storage density of the system [24], ii) the high turning temperature of the carbonation reaction [25], which allows using high-efficiency power cycles, and iii) the low cost, wide availability and non-toxicity of natural calcium oxide (CaO) precursors such as limestone and dolomite.

The so-called Electrical Energy Storage – Calcium looping (EES-CaL) system relies on using the power produced from a PV plant to provide heat by Joule effect for carrying out the calcination endothermic reaction, whose products CaO and CO_2 can be stored separately for long periods. When energy is required, the stored products are sent to another reactor where by means of the carbonation exothermic reaction is released the stored energy in the chemical bonds. The system is connected to the centralized power system to export electrical power generated in the power block for the discharge of the cycle. Thermal to electrical efficiencies higher than 40% can be reached in the integration of the CaL process in CSP plants [26]. The EES-CaL system allows exploiting several storage management strategies by just configuring the charging and discharging cycles of the TCES and integrating them with the electrical supplier system (PV plant) and the power system.

Despite that converting electric power to thermal would seem counterproductive from a thermodynamic point of view, there are several ambitious projects, such as the Google's Project Malta [27], which explores this possibility as alternative to batteries. Storing electricity in the form of heat is gaining momentum in the last years due to the very low prices of electricity production achieved in PV plants and the increasing surplus of electricity produced that cannot be used. Just in California 10 GWh of wind and solar generation is being wasted over the 24-hour period due to curtailment [28].

The aim of the present work is evaluating the potential of the PV-CaL integration as large scale storage system. A conceptual integration model is proposed for simulate the system behavior under several whether conditions. This document is structured as follows: firstly, the novel concept for EES based on CaL technology (EES-CaL) is described with focus on the PV integration (PV-CaL). Later, the system is simulated to analyze the daily behavior for each month of the year. The main results obtained are discussed highlighting the importance of properly managing the storage tanks. A brief discussion on economic issues is also introduced to complete this first approach to the EES-CaL concept.

2. Conceptual thermochemical energy storage system

Figure 1 illustrates the conceptual scheme for the EES-CaL integration. The system is composed by two well-differentiated and independent charging and discharging cycles with solid storage tanks and CO_2 vessel. The CaL process scheme is based on [29], where interested readers can find further details on the configuration. The EES–CaL process begins by activating the charging cycle, where the endothermic calcination of limestone ($CaCO_3$) takes place. During the charging cycle, electric power from PV is transformed to thermal power by electric heaters coupled to the calciner. Thus, a part of the electrical power generated in the PV system feeds the EES. The calciner, which may be configured as a Fluidized Bed (FB) or as an Entrained- Flow (EF) reactor, operates under atmospheric pressure at 950 ºC to ensure fast decomposition of $CaCO_3$ [23]. Thermal power provided to the calciner is used for increasing the solids temperature up to the reaction conditions and to provide the calcination enthalpy according to Eq 1.

$$CaCO_{3\,(s)} \rightarrow CaO_{(s)} + CO_{2\,(g)} \qquad \Delta H_r = 178\, kJ/mol \tag{1}$$

The $CaCO_3$ entering the calciner is controlled depending on the power provided by the PV system. The higher the power to the calciner the higher amount of $CaCO_3$ entering the reactor from the solids storage tank. The CaO produced during calcination is directly stored while the CO_2 is passed through a heat exchanger before being compressed. First, the CO_2 is sent to a cyclonic gas-solid preheater where $CaCO_3$ entering the reactor is heated. These preheaters are a well-known technology in cement plants [30]. Later, the CO_2 is sent to a heat recovery within a power cycle (e.g. Stirling Engine). Another option could be using its sensible heat for thermal applications within the plant. The CO_2 stream is further cooled before pressurizing it up to 75 bar by means of an intercooling compressor [31]. The charging cycle ends once the CaO and CO_2 streams produced in the calciner are stored.

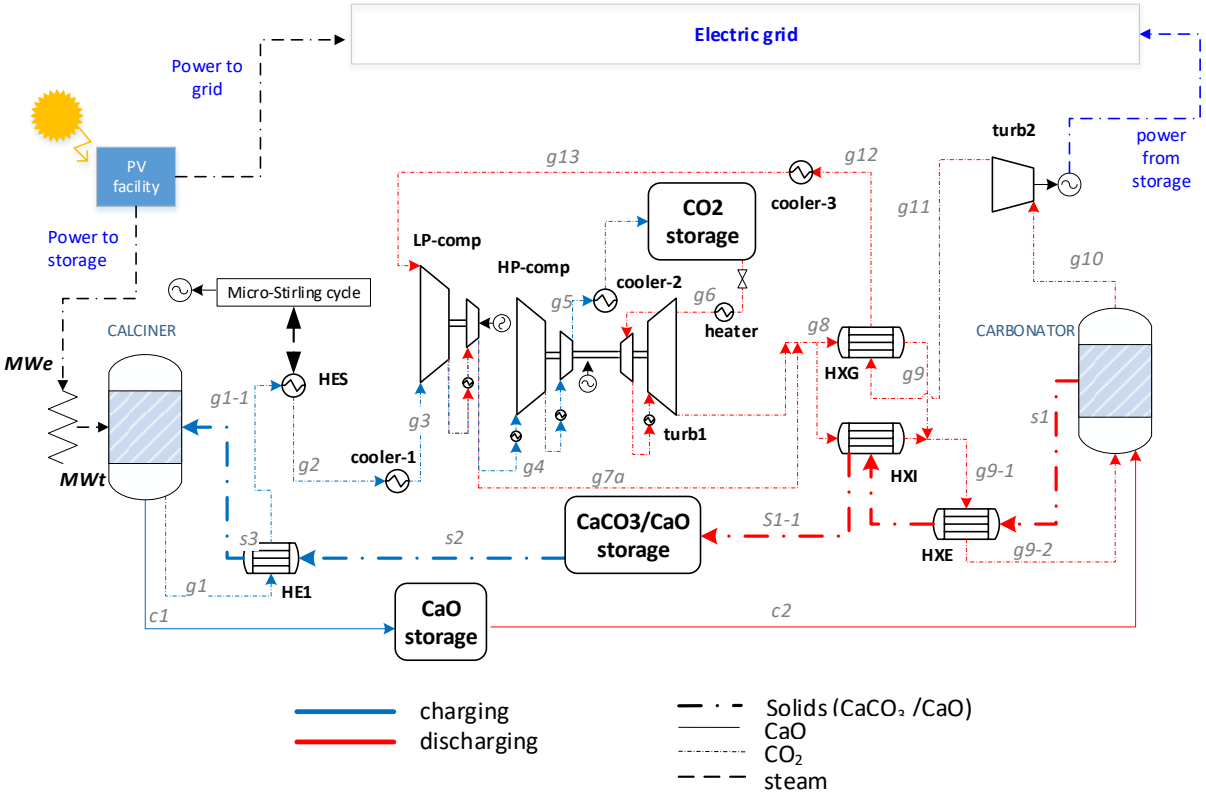

Figure 1. Conceptual scheme for PV-CaL. Process integration based on [29]

The $CaCO_3$ produced in the carbonator is stored to start a new cycle. The discharging cycle begins when there exists an interest in generating electrical power. To activate the discharge, CO_2 and CaO from the storage are sent to the carbonator reactor, where the exothermic carbonation reactions occurs. To achieve the desired operation at the exothermic reactor, the control system acts over the mass flow rate of CaO exiting the storage tank, which is an independent variable as input for the discharge cycle. In turn, the CaO mass flow rate entering the carbonator determines the total flow rate of CO_2 coming from the storage vessel. The CO_2 at low temperature is passed through a heater before passing it to a turbine to match the carbonator pressure (plus the pressure losses in the CO_2 heat exchangers). After this, the CO_2 stream is passed through a heat exchanger network in order to enter the carbonator at the highest temperature (Figure 1). The amount of CO_2 entering the carbonator is well above the stoichiometric need which allows using the non-reacting CO_2 as heat carrier fluid. As shown in Figure 1, the CO_2 exiting the carbonator at high temperature and pressure and evolves through a thermal turbine to produce power. In this direct integration the whole system, including charge and discharge processes, constitutes a closed CO_2 Brayton regenerative cycle with elements decoupled in time.

One of the main challenges of CaL process in the progressive CaO deactivation as the number of cycles increases. Previous works have shown however that CaO deactivation is highly dependent on the conditions in the calciner and carbonator reactors (temperature, total pressure, CO_2 partial pressure) as well as on the CaO precursor and their physical properties (particles size, impurities, etc.) [32], and they depend on the application. Thus, a residual CaO conversion as large as X=0.5 may be achieved for carbonation under a pure CO_2 atmosphere and calcination at 725 ºC in absence of CO_2 for natural limestone with particle size smaller than 45µm [33]. For larger particles, pore plugging limits conversion leading to a residual conversion around X=0.2. [34]. A conservative baseline value of X=0.15 is assumed in the

present work for simulating the PV-CaL integration at stationary conditions. Other assumptions on the CaL process scheme have been considered in this work. Calcination conversion is assumed as complete [35]. All gas-gas heat exchangers are modelled assuming a minimum temperature difference (DT) of 15ºC. Solid-gas heat exchangers are assumed in co-flow arrangement with the same exit temperature of both streams [29]. Solids conveying power consumption is assumed as 20MJ/ton [36]. Auxiliaries power consumption for cooling and heating are assumed as 0.8% of the thermal power. Turbomachinery efficiency, pressure drops values as well as other assumptions are presented in [29]. Weather information for the simulations has been taken from a typical year data [37]. Hourly simulation has been carried out without considering off-design conditions at this preliminary stage.

3. Case of study

A model of an integrated PV-CaL system is developed and simulated in this section.

3.1. Solar photovoltaic facility

A detailed simulation of a PV facility located in Seville (Spain) has been performed by using System Advisor Model (SAM) [37]. The PV system is sized for generating 20 MW in DC under 1,000 W/m^2 of total irradiance and cell temperature of 25 ºC. The PV module selected for the PV system is *Sun Power SPR-E19-245* (main characteristics are presented in Table 1) while the selected inverter is *SAM America: CS750CP-US-342V (*Table 2).

Table 1. Module characteristics at reference conditions

Nominal Efficiency	19.169	%
Maximum power (Pmp)	245.025	W_{dc}
Maximum power voltage (Vmp)	40.5	V_{dc}
Maximum power current (Imp)	6.1	A_{dc}
Open circuit voltage (Voc)	48.8	V_{dc}
Short circuit current (Isc)	6.4	A_{dc}
Module area	1.244	m^2

Table 2. Inverter characteristics at reference conditions

Maximum AC power	770000	W_{ac}
Maximum DC power	785145	W_{dc}
Power consumption during operation	1992.12	W_{dc}
Power consumption at night	364.7	W_{ac}
Nominal AC voltage	342	V_{ac}
Maximum DC voltage	1000	V_{dc}
Maximum DC current	1600	A_{dc}
Minimum MPPT DC voltage	545	V_{dc}
Nominal DC voltage	617.789	V_{dc}
Maximum MPPT DC voltage	820	V_{dc}
European weighted efficiency	98.122	%

A total number of 26 inverters is required for the system size, 20 MW_{dc}, with a maximum DC power by inverter of 785.14 kW_{dc} (Table 2). Thereby the DC-AC ratio would be 99.9% at reference conditions. The number of PV modules series-connected (modules per string) is given by the average DC voltage in the inverter (772.5 V_{dc}) and the V_{oc} of modules (Table 1). Thus, a total of 16 modules per string have been calculated for the system. The maximum

number of parallel strings is calculated as the maximum DC current divided by the short circuit current in the PV module (I_{sc}). As a result, a maximum of 6500 strings in parallel is obtained. Considering 20MW_{dc} of sizing power of the system and a configuration with 16 modules per string, a total of 5100 strings in parallel are required, resulting in 81600 modules. The final configuration of the system and main parameters at reference conditions are shown in Table 3:

Table 3. PV Power Plant configuration at reference conditions

Modules			Inverters		
Nameplate capacity	19994.04	kW_{dc}	Total capacity	20020	kW_{ac}
Number of modules	81600		Total capacity	20413.77	kW_{dc}
Modules per string	16		Number of inverters	26	
Strings in parallel	5100		Maximum DC voltage	1000	V_{dc}
Total module area	101510.4	m^2	Minimum MPPT voltage	545	V_{dc}
String V_{oc}	780.8	V	Maximum MPPT voltage	820	V_{dc}
String V_{mp}	648	V	Actual DC to AC ratio	99.9%	

The operation of this PV facility has been simulated for one-year. It results in an annual generation efficiency of 18.16%, with annual solar irradiance of 180.44 MWh/year and annual generation of 32.77 MWh/year. Figure 2 shows the results of the simulation along the year (a) and in the peak power day (b).

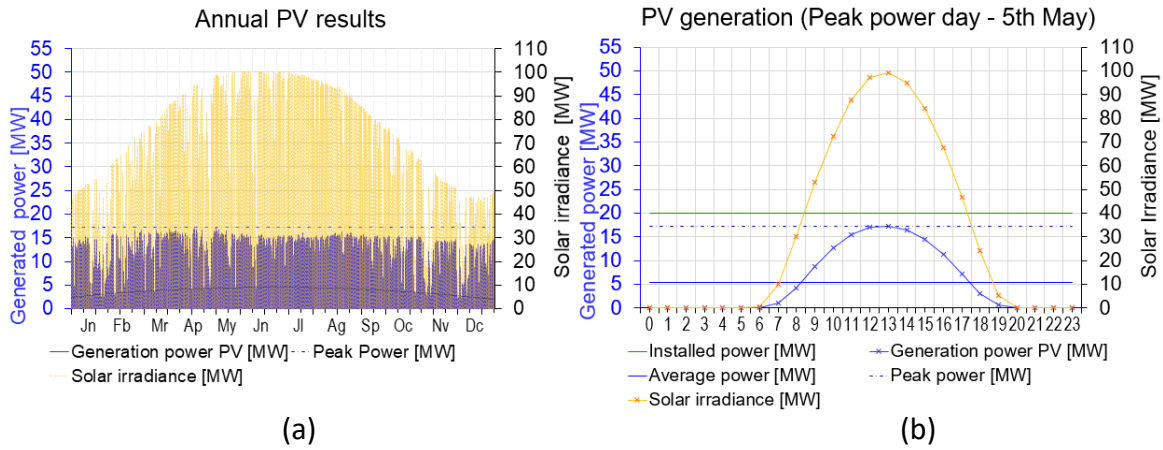

Note the scales difference between left and right vertical axes.

Figure 2. Simulation results: a) Annual results b) Peak power day results

Figure 2 shows the characteristic intermittent power production linked to seasonal and daily intermittence in solar resource. The PV facility is designed for 20 MW modules capability (under reference conditions), but peak power for the simulated year is 17.3 MW (Figure 2 (a)) since reference conditions and 1000W/m^2 of solar irradiance (nominal conditions) have not been achieved simultaneously to generate 20MW of PV power. The power generation average value is 3.74 MW, which is equivalent to 1638 full-load-hours throughout the year.

3.2. Base case simulation

The PV-CaL integration schematized in Figure 1 has been simulated in order to assess its potential as electric energy storage system. TCES process calculations have been carried out by using the commercial software ASPEN PLUS^{TM}. First, a base case is defined. It uses 5 MW_e of electric power produced by the PV system in the CaL process. In the charging period,

the use of electric heaters coupled to the calciner allows the calcination of 1.86 kg/s of $CaCO_3$. Taking into account that CaO conversion in the carbonation is not complete, in addition to $CaCO_3$, a certain amount of non-reacted CaO from the carbonator enters the calciner and therefore the total amount of solids would be 7.74 kg/s. For the base case analysis, it is assumed that solids exit the storage vessel at 690 ºC. Once calcination occurs, 0.82 kg/s of CO_2 and 6.93 kg/s of CaO are sent to their respective storage tanks. Within this base case, the discharging process is modelled assuming that all the previously stored CaO is sent to the carbonator for power production. However, in a daily process simulation the mass flow of products sent to the calciner for energy storage and to the carbonator for energy release will depend on the production strategy. Since the process is configured as energy storage system, different "charging" and "discharging" operation modes are considered. For simplicity, the plant efficiency is calculated as a weighted average of the results in both charging and discharging steps. Thus, the overall plant efficiency can be calculated according to Eq. 2 [29]:

$$\eta = \frac{\dot{W}_{net,charge}\,\Delta t_{charge} + \dot{W}_{net,discharge}\,\Delta t_{discharge}}{\dot{Q}_{PV}\,\Delta t_{charge}} \tag{2}$$

Where $\dot{W}_{net,charge}$ and $\dot{W}_{net,discharge}$ are the new electrical power consumed/produced in the charging and discharging periods respectively, Δt_i is the time working in the i-operation mode and $\dot{Q}_{PV}$ is the electric power coming from the PV facility. $\dot{W}_{net}$ in both charge and discharge steps is calculated as:

$$\dot{W}_{net} = \dot{W}_{turb,1} + \dot{W}_{turb,2} + \dot{W}_{stir} - \dot{W}_{HP-COMP} - \dot{W}_{LP-COMP} - \dot{W}_{PSOLCAL} - \dot{W}_{PSOLCAR} - \dot{W}_{AUXPOWCA} \tag{3}$$

Where $\dot{W}_{turb,1}$, $\dot{W}_{turb,2}$, and $\dot{W}_{stir}$ are the power produced in the turbine *TURB1*, *TURB2* and Stirling Engine respectively (Figure 1). $\dot{W}_{HP-COMP}$ and $\dot{W}_{LP-COMP}$ are the power consumed by the compressors while $\dot{W}_{PSOLCAL}$, $\dot{W}_{PSOLCAR}$ and $\dot{W}_{AUXPOWCA}$ are the power consumed for solids conveying in the calciner and carbonator sides and the power for heat auxiliaries respectively. Interested readers are referred to [29] for further information about the energy balance calculation.

Table 4 and 5 shows the main streams data and the energy balance results. Nomenclature corresponds to the one used in Figure 1.

Table 4. Main streams data for the PV-CaL integration (base case, 5 MWe from PV to CaL storage)

ID	P [bar]	T [^{0}C]	$\dot{m}$ [kg/s]	ID	P [bar]	T [^{0}C]	$\dot{m}$ [kg/s]
s1	3.5	900	7.74	**g5**	75.75	123.65	0.82
s1-1	1.14	689.20	7.74	**g5-2**	75	25	0.82
s2	1.14	689.60	7.74	**g6**	74.25	130	0.82
s3	1.11	719.69	7.74	**g7a**	3.85	78.36	18.01
c1	1	950	6.93	**g8**	3.85	76.80	18.83
c2	1	950	6.93	**g9**	3.66	702.62	18.83
g1	1	950	0.82	**g10**	3.5	900	18.02
g1-1	0.97	719.76	0.82	**g11**	1	718.18	18.02
g2	0.97	70	0.82	**g12**	0.95	91.99	18.02
g3	0.96	40	0.82	**g13**	0.94	40	18.02

The CO_2 stream exits the calciner at high temperature (950 ºC). This high temperature stream is used to increase the temperature of the incoming solids up to 720 ºC and to produce extra power through the integration with a thermal engine (i.e. Stirling) aiming to increase the global cycle efficiency and reducing the cooling demand of the system. After cooling, the CO_2 stream is compressed up to 75.75 bar before entering the storage tank. Once calcination take places, both the CO_2 and CaO streams previously produced in the calciner are sent to the carbonator reactor. In the discharging step, CO_2 at 75 bar and 25ºC is circulated through a heater increasing its temperature up to 130 ºC before passing through the secondary CO_2 turbine. After passing through the heat exchanger network, this stream arrives the carbonator at 753ºC.

Table 5. Energy balance for the PV-CaL integration (base case, 5 MW_e from PV to storage)

	Parameter	Charging step	Discharging step
	Solar thermal power (MW_{th}) from PV to storage $\dot{Q}_{PV}$	5	0
Heat exchangers thermal Power (MW_{th})	HES	0.58	-
	HE-1	0.23	-
	COOLER-1	-0.02	-
	HP-COMP (intercooler)	-0.25	-
	COOLER-2	-0.22	-
	HEATER	-	0.23
	TURB1 (interheater)	-	0.08
	COOLER-3	-	-0.84
	HXG	12.41	12.41
	HXE	1.17	1.17
	HXI	0.50	0.50
	LP-COMP (intercooling)	-	-1.23
Power inlet (MW_e)	CO_2 storage turbine (TURB1)	-	0.11
	Main CO_2 turbine (TURB2)	-	4.02
	Externally heated engine-Stirling engine (STIR)	0.12	-
	CO_2 storage compressor (HP-COMP)	-0.29	-
	Main CO_2 compressor (LP-COMP)	-	-1.84
	Auxiliaries heat calciner (AUXPOWCA)	-0.004	-
	Auxiliaries solids transport calciner (PSOLCAL)	-0.08	-
	Auxiliaries solids transport carbonator (PSOLCARB)	-	-0.08
W_{net}	$\dot{W}_{net,charge}$ (MWe)	-0.25	-
	$\dot{W}_{net,discharge}$ (MWe)	-	2.21
	Overall plant efficiency (η)	**39.21%**	

Table 5 includes main results from the energy balance in the plant. It shows that with the integration 14.66 MW_{th} have been recovered from the hot streams and integrated into the process, thus increasing the overall efficiency of the plant. Otherwise, there is still a need for extra cooling and heating power of 2.56 MW_{th} and 0.31 MW_{th} respectively. Global generation in the system is 4.25 MW_e by means of two CO_2 turbines allocated in the discharging cycle and an externally heated engine (for this size a Stirling engine is considered) that recovers thermal power from the hot CO_2 stream exiting the calciner. Energy consumption in the plant (2.28 MW_e) is mainly due to compressors consumption (2.12 MW_e). Note that net energy in the charging process is negative because of the CO_2 compression. As a result of this energy balance, the net generation in the charging and discharging cycle are 2.21 MW_e (net

generation) and -0.25 MW_e (net consumption), respectively when the solar thermal power entering in the calciner is 5 MW_e. Considering net electric generation in the system for a given thermal power entering the charging cycle, the overall efficiency of the system is 39.21%.

4. Process design

Once the PV-CaL process configuration has been analyzed for the base case, this section aims at studying the daily behavior of the system by considering a quasi-stationary simulation in an hourly basis. PV generation in a typical monthly day (hourly generation considered as the average value of hourly generation for every day of the month) is used as representative of the month behavior. Power generation in the PV facility is exported to the grid with a maximum power of 2.5 MW_e. When generation exceeds this limit, the surplus electricity is sent to the CaL charging cycle to initiate calcination and storage of reaction products.

In the analysis, a 24h constant discharging -power production- strategy is considered. Thus, the amount of constant power production from storage in each day depends on weather conditions. The surplus electricity generated in the PV facility over the exported to the grid is used for the charging cycle of the storage system. The amount of CaO and CO_2 used to produce surplus generation hours is distributed along the day to balance levels in the daily operation. Figure 3(a) summarizes the energy balance in the PV-CaL system. As result of the energy storage process along a typical July day, energy is stored for 11 hours, -from 9:00 to 19:00h- and then power production continues almost constant the rest of the day. Net generation during charging hours in the CaL system is negative because of the CO_2 compression (Table 5). Nevertheless, the net generation during discharging hours remains constant at 2.48 MW_e.

The PV-CaL system net generation takes into account net generation during discharging hours and PV exported during charging hours. This result is the total energy exported to the grid from the integrated PV-CaL system.

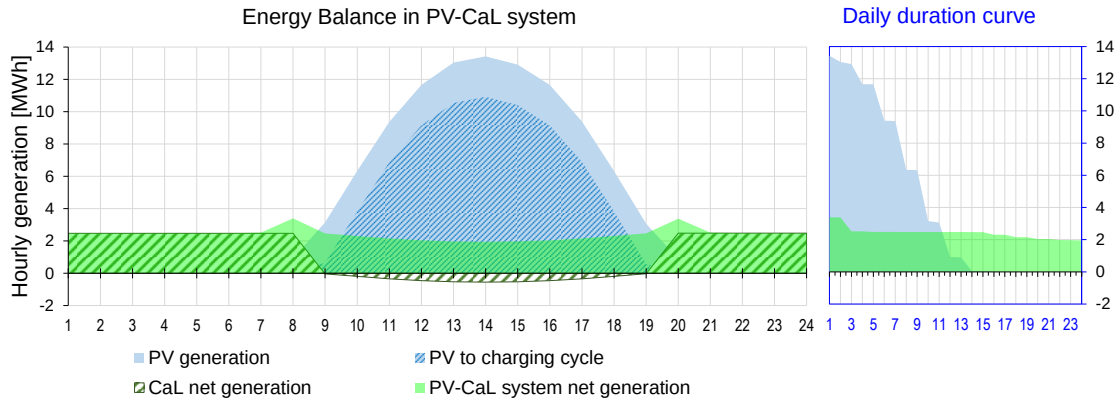

Figure 3. PV-CaL system performance: a) Energy balance in the PV-CaL system. Hourly results; b) Daily duration curve

The performance of the CaL system obtained is the same than in the base-case, 39.2% (Table 5), since all products from calcination are used in the carbonator. Otherwise, the global performance of the system, which is calculated as the PV-CaL net generation divided by the total PV-generation, is 56.5% and represents a loss of a 43.5% of the total PV-generation due to the storage system. These values are of the same order of magnitude than those reported by

Li et al. for a methanol-based thermochemical system integrated in a PV plant (41-43%) [21,38]. The CaL process efficiency (39.2% in this case) can be increased by an optimized configuration to reach values around 45-46% [23] with the consequent increase of the storage system global performance. To this end an energy-optimized integration and the proper selection of the reactor conditions (pressure, temperature, composition) are fundamental [23]. Remarkably, the CaL process performance can be substantially improved by mitigating the decay of CaO activity with the number of cycles (a conservative value of CaO residual conversion X=0.15 is assumed in this paper). Many studies are currently being focused on the search for methods to enhance the CaO multicyclic conversion [39].

Figure 3 (b) shows a plot the daily duration curve of the PV facility and the PV-Cal system and illustrates the purpose of this strategy, which is conceived to shift intermittent RES generation into almost even and controlled generation.

Storage tanks management is a crucial issue of the PV-CaL system. Figure 4 shows the daily evolution of solids ($CaCO_3$ + CaO), CaO and CO_2 tanks. According to the results, storage capacities of around 360 tonnes of CaO and 45 tonnes of CO_2 are needed.

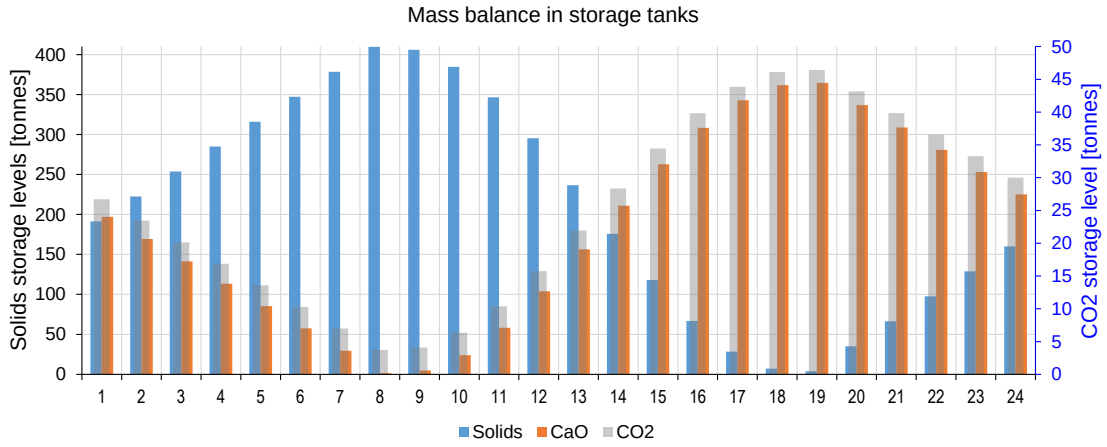

Figure 4. PV-CaL performance. Mass balance in storage tanks

Table 6 shows main results of the daily simulation for each month. 24 hours constant production is in the range of 2.48 MW_e in July to 1.19 MW_e in December, with an annual average of 1.85 MW_e. This average value is selected as design power production value to evaluate operation of the system throughout the year.

Table 6. Base PV-CaL generation. Monthly results

Month	Power generation [MW]		Energy balance - Generation [MWh]				Global PV-CaL performance	
	PV threshold	PV-CaL discharge	PV to grid)	PV to storage)	CaL to grid	PV-CaL system to grid	C/D [h]	Operation Performance
JAN	1.35	1.33	12.18	45.06	17.69	29.87	9/15	52.17%
FEB	1.5	1.47	14.28	49.98	19.60	33.88	9/15	52.72%
MAR	2.1	2.04	21.56	69.08	27.07	48.63	9/15	53.65%
APR	2	1.91	22.46	60.53	23.72	46.18	10/14	55.65%
MAY	2.3	2.30	26.97	67.71	26.53	53.5	11/13	56.50%
JUN	2.25	2.20	26.87	64.60	25.33	52.2	11/13	57.07%
JUL	2.5	2.48	29.40	72.83	28.55	57.95	11/13	56.69%
AGO	2.45	2.46	27.98	72.41	28.38	56.36	11/13	56.14%
SEP	1.95	1.88	20.66	63.79	25.01	45.67	9/15	54.08%
OCT	1.7	1.69	16.78	57.17	22.41	39.19	9/15	52.99%
NOV	1.2	1.19	10.66	42.87	16.81	27.47	8/16	51.31%
DEC	1.2	1.19	10.31	42.45	16.63	26.94	8/16	51.06%

5. Daily simulation

When the system is simulated on a representative day of December, the amount of products from the charging cycle is enough to allow generating 1.85 MWe almost constant during 19h, achieving a global efficiency in the operation of the system of 54.59% (Figure 5).

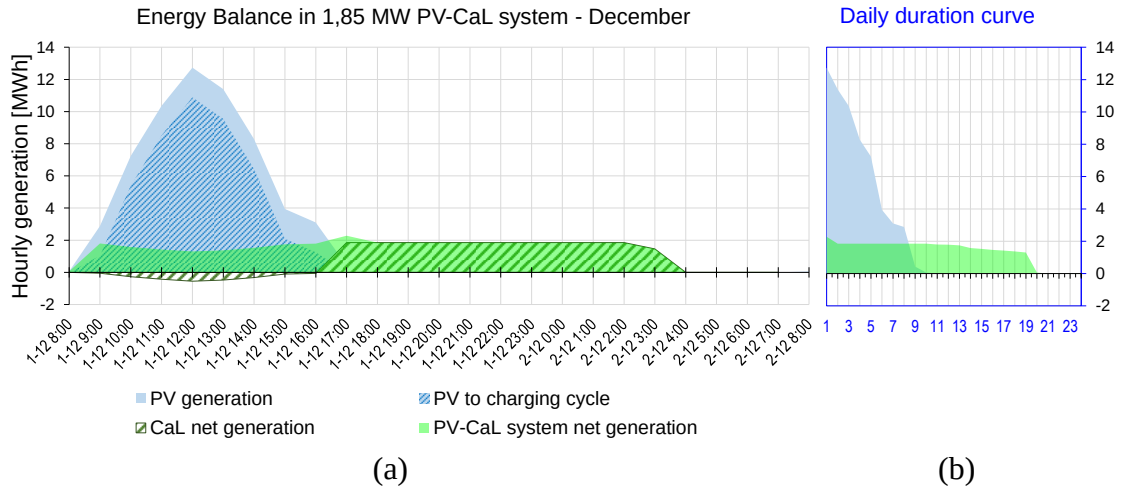

Figure 5. PV-CaL 1.85MWe system – December: a) Energy balance in the PV-CaL system; b) Daily duration curve

Figure 6 shows the evolution of storage tanks levels along the simulated period. In this case, calcination products are fully consumed along the day and the system is balanced on a daily basis. This is the strategy set for this application but different ones can be considered taken into account the seasonal storage capacity of the CaL system. The minimum required storage capacities are 251.52 tonnes for solids, 26.49 tonnes for CO_2 and 225.03 tonnes for CaO.

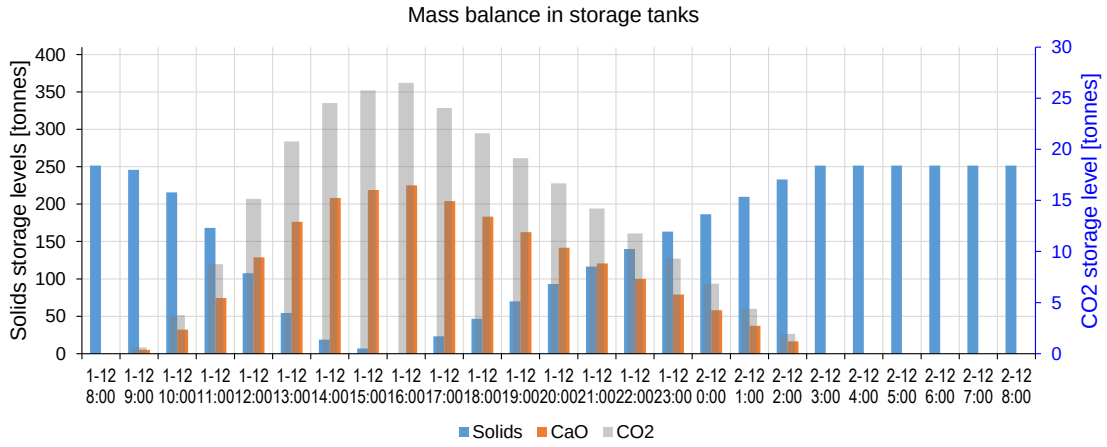

Figure 6. CaL 1.85MWe system – December. Mass balance in storage tanks

The opposite scenario is found on a representative of July (with a peak power capacity of 115.68 MWh/day). Figure 7 shows the performance of the system in this month. During the charging cycle (1 Jul/9h -1 Jul/19h) 454.56 tonnes of CaO are produced and stored before the discharging cycle (1 Jul/20h -2 Jul/8h), which consumes 244.04 tonnes of CaO, thus implying the necessity of extra-storage to address decoupled values of solids and gas streams production and consumption to maintain a strategy of constant power along the whole day. Figure 8 shows the mass balance in the PV-CaL system during the operation day. Calcination products are not totally consumed while the consumption of $CaCO_3$ in the calciner is not totally replaced in the discharging cycle thus reducing the level of solids storage tank at the end of the operation day. This is because the selected operation strategy, which must be improved in order to minimize the storage size, and therefore the investment cost.

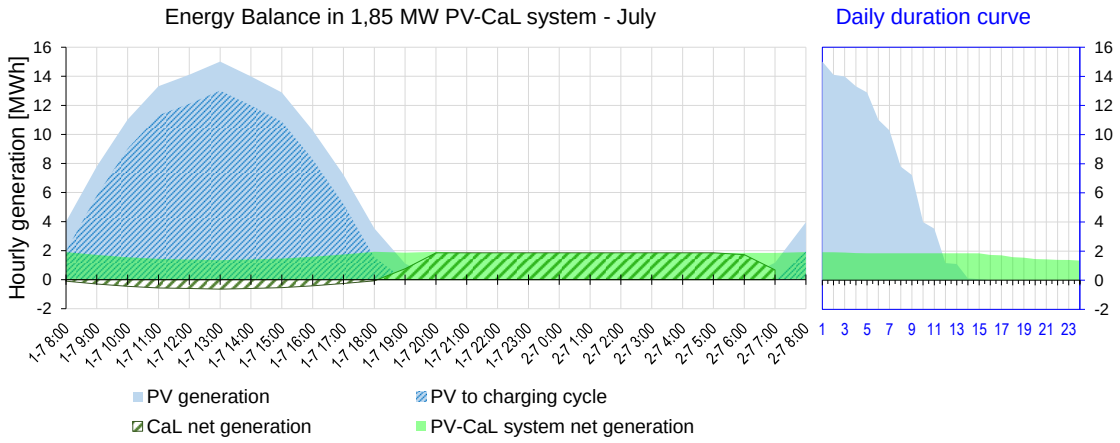

Figure 7. PV-CaL 1.85MWe system – July: a) Energy balance in the PV-CaL system; b) Daily duration curve

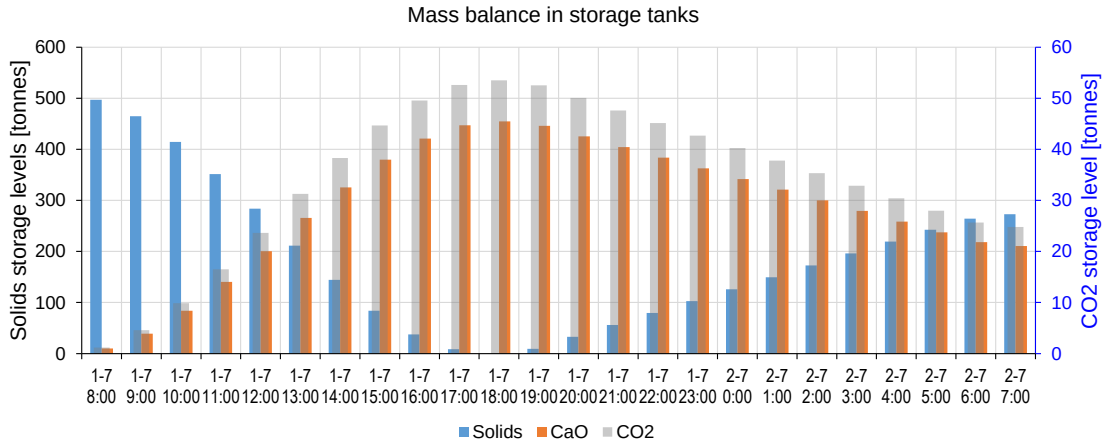

Figure 8. CaL 1.85MWe system – July. Mass balance in storage tanks

6. Economic and sustainability notes

A brief economic study has been carried out for the PV system simulated in the previous section. For storage system sizing the date of first of July has been selected. The aim of this section is to show the potential of the PV-CaL conceptual integration. According to the daily behaviour simulation, 91.18MWhe from the PV facility are charged in the storage system.

In order to estimate the PV-CaL system cost, the methodology proposed in [40] has been followed. Process equipment capital cost has been calculated by using Aspen Capital Cost Estimator [41]. Capital costs of the calciner and carbonator reactors have been estimated according to [42]. Table 7 shows the capital cost estimation for the CaL process as TCES. Because of the novelty of the application and the design effort at this stage, a high contingency cost for the process (15%) and project (30%) has been assumed [40]. The owner cost, which includes feasibility studies, insurance, permitting, land, etc. has been estimated from [41]. Table 8 shows investment costs. For comparison, a generic batteries-based system is considered for the same size than the PV-CaL system. According to [9], the installed cost (including battery cells -whose cost is around 300-550$/kWh-, a power conversion system, a battery management system, etc.) of a Li-ion battery storage system currently available in the market is around 1200$/kWh, which yields a total cost for the simulated case of 109M€.

Table 7. Capital cost estimation for the proposed EES-PV-CaL configuration

Process equipment [M€]	25.28
Reactors	*12.03*
Storage Vessels	*2.77*
Heat exchangers	*2.45*
Turbomachinery	*5.95*
Solids conveying and separation	*0.47*
Electric heaters	*0.65*
Micro steam cycle	*0.96*
Supporting facilities [M€]	13.65
Piping	*3.09*
Civil	*0.62*
Steel	*0.13*
Instruments	*2.62*
Electrical	*1.98*
Insulation	*0.33*
Paint	*0.17*
Bare Erected Cost (BEC) [M€]	**38.93**
Engineering services [43] [M€]	1.75
Engineering, Procurement and Construction (EPC) cost [M€]	**40.68**
Process contingencies [40] [M€]	6.1
Project contingencies [40] [M€]	12.2
Total plant cost [M€]	**58.98**
Owner cost [M€]	1.18
Total Overnight Cost (TOC) [M€]	**60.16**

As may be seen in Table 7, a notable cost reduction could be achieved by using the PV-CaL instead of the batteries-based PV. It shows the interest for further studies of this application at large scale level. As a novel technology, uncertainty about costs evolution for the EES- PV-CaL plant is high. To include into the analysis this uncertainty, a sensitivity analysis with random numbers has been carried out by considering a typical range of potential values for the main costs. Several values can be found in the literature for process and project contingencies for a CaL-based system [44,45]. Thus, a normal distribution for the process equipment cost (μ=25;σ=3) and uniform distribution for both process contingencies ([7-20%]) and project contingencies ([20-40%]) was considered. The sensitivity analysis results are shown in Figure 9.

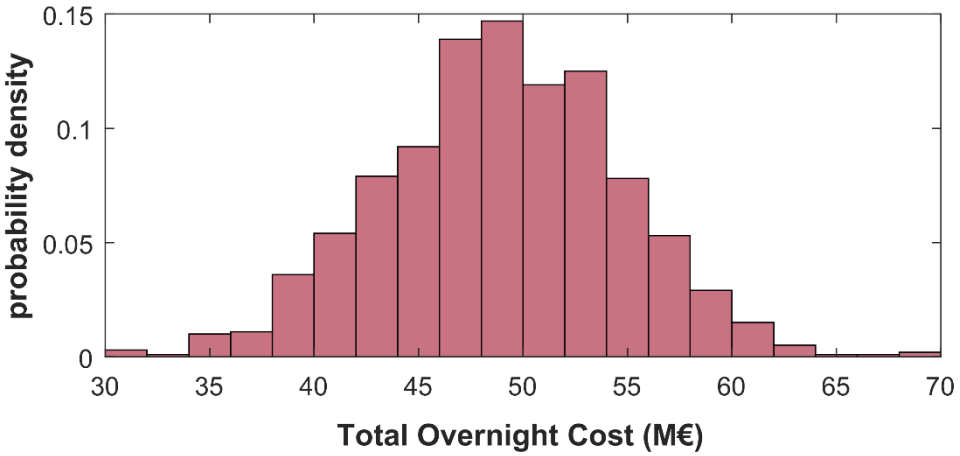

Figure 9. Total Overnight Cost (TOC) obtained from a sensitivity analysis base in random numbers.

According to the obtained results, the specific total overnight cost estimated is higher than values previously published about CaL as post-combustion CO_2 capture system at large scale (~500-600MWe), which are around 1700-3000€/$KW_{e,gross}$ [46,47]. This is mainly because of the system size, since post-combustion CO_2 capture system are two order of magnitude higher than the PV-CaL system analyzed in the present work. Moreover, in the PV-CaL the cost of the storage size is higher to ensure proper dispatchability. Nevertheless, as shown in Figure 9, the estimated investment cost is notably lower than the expected cost for electrochemical batteries (109M€).

The proposed concept has a number of relevant advantages for large scale development. It is based on natural CaO precursors (such as limestone), which are among the most abundant materials in Earth. Thus, the raw material employed is widely available, non-toxic, abundant and cheap (~10 $/ton). This highly influences the variable O&M costs of the plant facing possible reposition or make-up [48] of material to the system. These essential characteristics for massive energy storage make the PV-CaL concept an attractive technology for the sustainable development of PV power plants without any expected raw material competition with other applications.

A more detailed economic analysis will be developed in a future work. This will include optimization of dispatchability strategies for several PV plant sizes by considering entire year operation, and the effect of this on the Return ON Investment (ROI). A detailed Operational Expenditures (OPEX) analysis will be fundamental in this case.

7. Conclusions

This manuscript presents a novel concept to integrate Thermochemical Energy Storage (TCES) systems using the Calcium-Looping (CaL) cycle in PV plant (PV-CaL system) for electrical energy storage (EES). The work is focused on assessing the operation of the TCES system to address a generation strategy. Different generation strategies could be applied to the system to increase dispatchability of the PV facility. As a first conceptual approach the analysis has been focused on operation of the storage system to keep a constant power generation while the PV generation is variable. The CaL system reaches an efficiency of 39.2% which is low compared to available batteries at large scale whose efficiencies are around 60-70%. Several strategies can be implemented to increase the CaL process efficiency,

such as optimizing energy recovery in the process, selecting optimum reactor conditions (pressure, temperature, composition, etc.) and improving the multicyclic CaO conversion. Despite this lower efficiency, the PV-CaL system presents some advantages that make it a very interesting option for sustainable and large-scale energy storage. The PV-CaL system is based on one of the most abundant materials available in nature (limestone, $CaCO_3$), which circumvents the risk of resource scarcity that may compromise the technical and economic viability of the storage system. This is one of the main advantages that this system presents over current solutions for EES based on chemical batteries. Batteries represent a suitable option for PV and wind storage; however, current materials used in commercial batteries (e.g. Li, Ni, Mn, Co) make them cost intensive whereas the amount of material needed for large-scale applications their storage capability. Another advantage of the integration of the PV-CaL system in the grid for large-scale energy storage is that power is generated mechanically in a CO_2 turbine, a rotatory thermal engine connected to an asynchronous generator that converts mechanical power into electricity (alternating current AC power). This inertial power system results crucial as the size of the system increases due to frequency stability required to the interconnected power grid. The power block and rest of required equipment is easily scalable at the commercial level: two solid-gas reactors (e.g. fluidized bed or entrained flow reactors); two solid storage tanks ($CaCO_3$ and CaO); a vessel to store the CO_2 stream in supercritical conditions (75 bar and ambient temperature); electric heaters; equipment for solids and gas conveying; instrumentation and control system; and auxiliary systems needed for the correct operation of the system. Regarding cost analysis, very conservative values were chosen for the CaL-based storage system because of its novelty. Despite this, the estimated cost is notably lower than the typical cost of batteries, which suggests a potential further cost reduction in the next years that would increase even more the PV-CaL competitiveness. From these results it can be inferred that the proposed PV-CaL concept is an attractive technology for large-scale storage of electric energy.

Acknowledgements

This work has been partially supported by the European Union's Horizon 2020 research and innovation programme under grant agreement No 727348, project SOCRATCES and by the Spanish Government Agency Ministerio de Economía y Competitividad (MINECO-FEDER funds) under contracts CTQ2014-52763-C2, CTQ2017- 83602-C2 (-1-R and -2-R).

References

[1] Sampaio PGV, González MOA. Photovoltaic solar energy: Conceptual framework. Renew Sustain Energy Rev 2017;74:590–601. doi:10.1016/j.rser.2017.02.081.

[2] International Energy Agency (IEA). 2018 Snapshot og global photovoltaic markets. 2018.

[3] (IEA) International Energy Agency. Trends 2016 in Photovoltaic Applications. Survey Report of Selected IEA Countries between 1992 and 2015. 2016.

[4] REN21. Renewables 2017: global status report. vol. 72. 2017. doi:10.1016/j.rser.2016.09.082.

[5] Jordehi AR. Parameter estimation of solar photovoltaic (PV) cells: A review. Renew Sustain Energy Rev 2016;61:354–71. doi:10.1016/j.rser.2016.03.049.

[6] Mundada AS, Shah KK, Pearce JM. Levelized cost of electricity for solar photovoltaic, battery and cogen hybrid systems. Renew Sustain Energy Rev 2016;57:692–703. doi:10.1016/j.rser.2015.12.084.

[7] Karimi M, Mokhlis H, Naidu K, Uddin S, Bakar AHA. Photovoltaic penetration issues and impacts in distribution network - A review. Renew Sustain Energy Rev 2016;53:594–605. doi:10.1016/j.rser.2015.08.042.
[8] Obi M, Bass R. Trends and challenges of grid-connected photovoltaic systems - A review. Renew Sustain Energy Rev 2016;58:1082–94. doi:10.1016/j.rser.2015.12.289.
[9] IRENA. Battery Storage for Renewables : Market Status and Technology Outlook. Irena 2015:60.
[10] Rydh CJ, Sandén BA. Energy analysis of batteries in photovoltaic systems. Part I: Performance and energy requirements. Energy Convers Manag 2005;46:1957–79. doi:10.1016/j.enconman.2004.10.003.
[11] Luo X, Wang J, Dooner M, Clarke J. Overview of current development in electrical energy storage technologies and the application potential in power system operation. Appl Energy 2015;137:511–36. doi:10.1016/j.apenergy.2014.09.081.
[12] https://www.tesla.com/es_ES/blog/Tesla-powerpack-enable-large-scale-sustainable-energy-south-australia?redirect=no n.d.
[13] Geth F, Brijs T, Kathan J, Driesen J, Belmans R. An overview of large-scale stationary electricity storage plants in Europe: Current status and new developments. Renew Sustain Energy Rev 2015;52:1212–27. doi:10.1016/j.rser.2015.07.145.
[14] Mahlia TMI, Saktisahdan TJ, Jannifar A, Hasan MH, Matseelar HSC. A review of available methods and development on energy storage; Technology update. Renew Sustain Energy Rev 2014;33:532–45. doi:10.1016/j.rser.2014.01.068.
[15] International Energy Agency (IEA). Technology Roadmap: Energy storage. 2014.
[16] Díaz-González F, Sumper A, Gomis-Bellmunt O, Bianchi FD. Energy management of flywheel-based energy storage device for wind power smoothing. Appl Energy 2013;110:207–19. doi:10.1016/j.apenergy.2013.04.029.
[17] Tixador P. Superconducting Magnetic Energy Storage : Status and Perspective. IEEE/CSC ESAS Euro Supercon News For 2008:1–14.
[18] Díaz-González F, Sumper A, Gomis-Bellmunt O, Villafáfila-Robles R. A review of energy storage technologies for wind power applications. Renew Sustain Energy Rev 2012;16:2154–71. doi:10.1016/j.rser.2012.01.029.
[19] Pardo P, Deydier A, Anxionnaz-Minvielle Z, Rougé S, Cabassud M, Cognet P. A review on high temperature thermochemical heat energy storage. Renew Sustain Energy Rev 2014;32:591–610. doi:10.1016/j.rser.2013.12.014.
[20] Prieto C, Cooper P, Fernández AI, Cabeza LF. Review of technology: Thermochemical energy storage for concentrated solar power plants. Renew Sustain Energy Rev 2016;60:909–29. doi:10.1016/j.rser.2015.12.364.
[21] Li W, Hao Y. Efficient solar power generation combining photovoltaics and mid-/low-temperature methanol thermochemistry. Appl Energy 2017;202:377–85. doi:10.1016/j.apenergy.2017.05.086.
[22] Li W, Ling Y, Liu X, Hao Y. Performance analysis of a photovoltaic-thermochemical hybrid system prototype. Appl Energy 2017;204:939–47. doi:10.1016/j.apenergy.2017.05.077.
[23] Chacartegui R, Alovisio A, Ortiz C, Valverde JMM, Verda V, Becerra JAA. Thermochemical energy storage of concentrated solar power by integration of the calcium looping process and a CO2 power cycle. Appl Energy 2016;173:589–605. doi:10.1016/j.apenergy.2016.04.053.
[24] Kyaw K, Matsuda H, Hasatani M. Applicability of carbonation/decarbonation reactions to high-temperature thermal energy storage and temperature upgrading. J Chem Eng Japan 1996;29:119–25. doi:10.1252/jcej.29.119.
[25] Barin I. Thermochemical data of pure substances VCH, Weinheim (1989) 1989.

[26] Alovisio A, Chacartegui R, Ortiz C, Valverde JM, Verda V. Optimizing the CSP-Calcium Looping integration for Thermochemical Energy Storage. Energy Convers Manag 2017;136:85–98. doi:10.1016/j.enconman.2016.12.093.
[27] The Moonshot factory. Project Malta: Storing renewable energy in molten salt n.d. https://x.company/projects/malta/ (accessed November 1, 2018).
[28] California ISO. Wind and Solar Curtailment April 28, 2018 2018.
[29] Ortiz C, Romano MC, Valverde JM, Binotti M, Chacartegui R. Process integration of Calcium-Looping thermochemical energy storage system in concentrating solar power plants. Energy 2018;155:535–51. doi:10.1016/j.energy.2018.04.180.
[30] Schorcht F, Kourti I, Scalet BM, Roudier S, Sancho LD. Best Available Techniques (BAT) Reference Document for the Production of Cement, Lime and Magnesium Oxide. 2013. doi:10.2788/12850.
[31] Ortiz C, Chacartegui R, Valverde JMM, Alovisio A, Becerra JAA. Power cycles integration in concentrated solar power plants with energy storage based on calcium looping. Energy Convers Manag 2017;149:815–29. doi:10.1016/j.enconman.2017.03.029.
[32] Perejón A, Miranda-Pizarro J, Pérez-Maqueda LA, Valverde JM. On the relevant role of solids residence time on their CO2 capture performance in the Calcium Looping technology. Energy 2016;113:160–71. doi:10.1016/j.energy.2016.07.028.
[33] Sarrion B, Valverde JM, Perejon A, Perez-Maqueda LA, Sanchez-jimenez PE. On the multicycle activity of natural limestone/dolomite for cheap, efficient and non-toxic Thermochemical Energy Storage of Concentrated Solar Power. Energy Technol 2016;4:1013–9. doi:10.1002/ente.201600068.
[34] Benitez-Guerrero M, Sarrion B, Perejon A, Sanchez-Jimenez PE, Perez-Maqueda LA, Manuel Valverde J. Large-scale high-temperature solar energy storage using natural minerals. Sol Energy Mater Sol Cells 2017;168:14–21. doi:10.1016/j.solmat.2017.04.013.
[35] Obermeier J, Sakellariou KG, Tsongidis NI, Baciu D, Charalambopoulou G, Steriotis T, et al. Material development and assessment of an energy storage concept based on the CaO-looping process. Sol Energy 2017;150:298–309. doi:10.1016/j.solener.2017.04.058.
[36] Edwards SEB, Materić V. Calcium looping in solar power generation plants. Sol Energy 2012;86:2494–503. doi:10.1016/j.solener.2012.05.019.
[37] National Renewable Energy Laboratory. Golden C. System Advisor Model Version 2017.1.17 (SAM 2017.1.17) n.d.
[38] Li W, Hao Y. Explore the performance limit of a solar PV – thermochemical power generation system. Appl Energy 2017;206:843–50. doi:10.1016/j.apenergy.2017.08.172.
[39] Perejón A, Romeo LM, Lara Y, Lisbona P, Martínez A, Valverde JM, et al. The Calcium-Looping technology for CO2 capture: On the important roles of energy integration and sorbent behavior. Appl Energy 2016;162:787–807. doi:10.1016/j.apenergy.2015.10.121.
[40] Rubin ES, Short C, Booras G, Davison J, Ekstrom C, Matuszewski M, et al. A proposed methodology for CO2 capture and storage cost estimates. Int J Greenh Gas Control 2013;17:488–503. doi:10.1016/j.ijggc.2013.06.004.
[41] Aspen Technology Inc. Aspen Capital Cost Estimator: User's Guide 2012:738.
[42] Romano MC, Spinelli M, Campanari S, Consonni S, Cinti G, Marchi M, et al. The calcium looping process for low CO2 emission cement and power. Energy Procedia 2013;37:7091–9. doi:10.1016/j.egypro.2013.06.645.
[43] Politecnico di Milano – Alstom UK (CAESAR project). European best practice

guidelines for assessment of CO2 capture technologies. 2011.
[44] Mantripragada HC, Rubin ES. Calcium looping cycle for CO2 capture: Performance, cost and feasibility analysis. Energy Procedia 2014;63:2199–206. doi:10.1016/j.egypro.2014.11.239.
[45] Cormos CC. Economic evaluations of coal-based combustion and gasification power plants with post-combustion CO2capture using calcium looping cycle. Energy 2014;78:665–73. doi:10.1016/j.energy.2014.10.054.
[46] Romeo LM, Abanades JC, Escosa JM, Paño J, Giménez A, Sánchez-Biezma A, et al. Oxyfuel carbonation/calcination cycle for low cost CO2capture in existing power plants. Energy Convers Manag 2008;49:2809–14. doi:10.1016/j.enconman.2008.03.022.
[47] Hanak DP, Manovic V. Economic feasibility of calcium looping under uncertainty. Appl Energy 2017;208:691–702. doi:10.1016/j.apenergy.2017.09.078.
[48] Romeo LM, Lara Y, Lisbona P, Escosa JM. Optimizing make-up flow in a CO2capture system using CaO. Chem Eng J 2009;147:252–8. doi:10.1016/j.cej.2008.07.010.